Journal of Engineering and Technology for Industrial Applications

ITEGAM-JETIA

Manaus, v.11 n.55, p. 154-160. September/October, 2025.
DOI: https://doi.org/10.5935/jetia. v.11 n.55.1959

ISSN ONLINE: 2447-0228

RESEARCH ARTICLE OPEN ACCESS

NUMERICAL STUDY OF THE ASYNCHRONOUS EXCITATION EFFECT OF BOUMERDES' EARTHQUAKE ON A BRIDGE BEHAVIOR

Guesmi Mohamed[1], Belkheiri Nassira[2] and Guesmi Mohamed Lakhder[3]

[1,2] Department of civil engineering, Faculty of sciences and technology, University of Djelfa, BP 3117, Djelfa, 17000, Djelfa, Algeria.
[3] Department of Civil Engineering and Hydraulic, Faculty of Sciences and Technologie, BP 401 Guelma 24000, Guelma, 10587, Algeria.

[1]http://orcid.org/0000-0002-1826-2485, [2]https://orcid.org/0000-0002-7390-847X, [3]https://orcid.org/0000-0003-1054-8005

Email: guesmi82@gmail.com, n.belkheiri@univ-djelfa.dz, gmlak2704@gmail.com

ARTICLE INFO

Article History
Received: May 5, 2025
Revised: May 30, 2025
Accepted: October 1, 2025
Published: October 31, 2025

Keywords:
Asynchronous excitation,
Bridge,
Earthquake,
Newmark method,
State-space method.

ABSTRACT

This work shows the numerical analysis of asynchronous excitation effects on a bridge response due to the Boumerdes earthquake, employing the finite element approach in modeling and the Newmark method for dynamic response analysis. The influence of the temporal delay of excitation between the supports on the reaction of the structure is investigated, and how these differences can change structural behaviour during seismic occurrences is studied. The dynamic displacements, normal and shear forces, and bending moments are estimated by comprehensive simulations. The obtained results reveal that, due to the non-uniformity in the earthquake excitation, there are changes in qualitative and quantitative aspects of the dynamic displacements of the bridges. This will subsequently subject the bridges to increasing displacements, hence harming their structural safety and integrity. The analysis further shows that, due to non-uniform seismic forces, the distribution of normal and shear efforts, combined with bending moments, generates large concentrations of stresses that were underestimated in uniform loading conditions. From these data, it can stress the necessity of non-uniform distribution of seismic loading during bridge design or evaluation. It provides essential insight for the engineers and designers who will execute the improvement in the seismic resistance of bridge constructions in earthquake areas.

I. INTRODUCTION

Dynamic analysis is required for structures subjected to random or dynamic loads. Essentially, dynamic analysis comprises response spectrum analysis and time history analysis. In case of structures with vast spans, the ground motion effects at various supports may vary. For such cases, time history analysis is essential to account for the time delay in earthquake ground motions. One of the new areas of recent research has been the influence of spatial variability in ground motion on bridge responses. Many such studies have pointed out that the incoherency in ground motion, wave-passage effects, and local site conditions all combine to produce significant variations in seismic input along the length of a bridge[1]. For instance, the authors in [2] investigated how such spatially varying motions result in more complicated stress distributions and deformation patterns in bridge structures.

Their work then indicated how the traditional seismic analysis, which is highly based on assumptions of uniform ground motion, misses complex responses when different parts of a bridge are subjected to different seismic forces. Nonlinear dynamic analysis has also been used to determine the behavior of bridges for multi-support seismic excitations. In this context, Sextos et al. [3] analyzed the nonlinear dynamic response of multi-span bridges and observed that neglecting the spatial variability of seismic inputs may result in underestimation of the stress in critical components such as piers and bearings. Their findings pointed to the important role of accounting for spatial variability in seismic design, to avoid structural underperformance or failure under seismic events. Other researchers have

sought an understanding of how, within spatially variable seismic inputs, the effect of SSI on bridges is considered. Hoseini et al. [4] illustrated that structure-soil interaction (SSI) significantly alters the seismic demands on bridge piers and abutments, especially when accounting for spatial variability. That is how the scientists' research pointed out that SSI, through the interaction of soil and structure, can enhance seismic forces, which is followed by increased deformation and distribution of stress than models without accounting for SSI effects.

In 2018, Yudakul and Ates [5] studied the performance of the lead rubber bearing (LRB)[6] isolator devices to reduce the seismic demand on bridges under multi-support ground motions. Through this study, it was observed that the performance of the isolating devices is significantly improved by the consideration of spatial variability and may provide a feasible way to solve the complex seismic response problems for these bridges. In 2021, Shen et al.[7] studied the effect of the ground motion spatial variability on the collapse behavior of buildings. Accordingly, a finite element model was put forward to simulate the collapse of the reinforced concrete (RC) structure, with four typical three-story buildings chosen for analysis. All these results indicate that the spatial variability in ground motion has an important impact on structural response and collapse mode, especially for higher earthquake intensity. Therefore, such variability should not be ignored in the simulation. Coupling of structural nonlinearity with randomness in the ground motion is one of the essentials behind collapse behavior.

In 2020, Ering and Babu[8] studied the effects of spatial variability in earthquake ground motions on the reliability of road systems crossing slopes susceptible to landslide failure. These models use the Material Point Method to model landslide-induced road failures by simulating the slope behavior under seismic loading. Further, the results show that the spatially varying seismic forces have significant effects on the slope failure risks. Neglecting these variations underestimates the landslide and road system risks. Critical variables, such as Arias intensity, hence determine slope displacement and the behavior of the landslides. Further, in 2024, Guesmi et al. [9] investigated the effectiveness of the state-space method to analyze multi-support excitation in a structure subjected to non-uniform seismic loading and thus proved considerably efficient and accurate as compared to traditional methods such as the Duhamel integral, the Newmark method, etc. It also points out the computational advantages of the state-space method in large structures where the computational speed may become critical.

The paper is organized as follows : an extensive background on previous studies that pinpoint the importance of the proposed subject is provided at the outset.This section focuses on the progress made in the interpretation of multi-support seismic excitations and their dynamic structural response. Then, the case that is studied is described in detail, while afterwards, the approach followed for the finite element analysis is presented in detail. Finally, it provides the results developed from the performed analyses, with their interpretation, giving information about the dynamic behaviour of structures under different seismic conditions. The paper finally wraps up by summarizing the conclusions drawn from findings and recommendations for future research.

II. PROBLEM DESCRIPTION

A time history analysis of a bridge comprising four frames is conducted to investigate its dynamic response under both uniform and non-uniform excitation scenarios. This analysis utilizes the finite element method, specifically employing the Newmark method for solving the governing equations of motion. The geometric dimensions of the bridge are detailed in Figure 1.a, where the beam cross-section measures 80 x 120 cm and the column cross-section is 80 x 80 cm. The material properties include a Young's modulus of E=2.48×106 Pa and a volumetric massρ=2402kg/m3, with a damping ratio of ξ=0.05. The seismic excitation is modeled based on the Boumerdès earthquake, which is depicted in Figure 1.b.

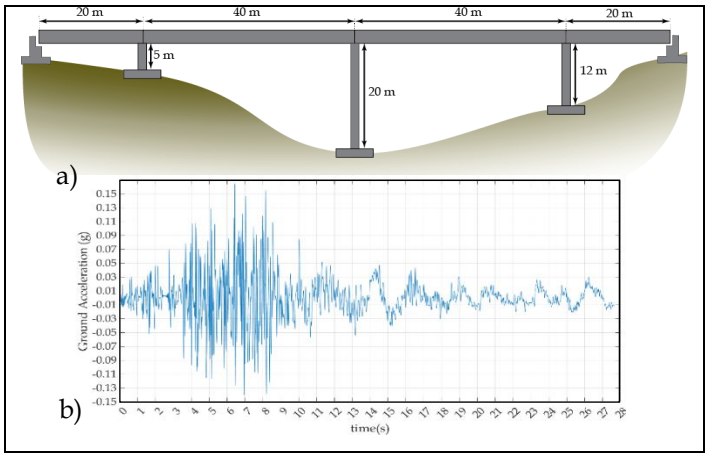

Figure 1: Problem description a) Bridge dimensions.
b) Acceleration of Boumerdès earthquake.
Source: Authors, (2025).

III. NUMERICAL FORMULATION

The motion equations for a multi-degree-of-freedom (MDOF) system subjected to multi-support excitations can be expressed as follows [10,11].

$$\begin{bmatrix} M_{ss} & M_{sg} \\ M_{gs} & M_{gg} \end{bmatrix} \begin{Bmatrix} \ddot{x}^t \\ \ddot{x}_g \end{Bmatrix} + \begin{bmatrix} C_{ss} & C_{sg} \\ C_{gs} & C_{gg} \end{bmatrix} \begin{Bmatrix} \dot{x}^t \\ \dot{x}_g \end{Bmatrix} + \begin{bmatrix} K_{ss} & K_{sg} \\ K_{gs} & K_{gg} \end{bmatrix} \begin{Bmatrix} x^t \\ x_g \end{Bmatrix} = \begin{Bmatrix} 0 \\ P_g \end{Bmatrix} \quad (1)$$

The mass matrix M_{ss} represents the mass associated with the superstructure and non-support degrees of freedom, while M_{gg} corresponds to the mass associated with the support degrees of freedom. The matrices $M_{sg}$and M_{gs} are coupling mass matrices that account for the inertial forces acting on the superstructure due to the movements of the supports. The damping and stiffness matrices are defined in a similar manner. The vector x^t denotes the total displacements related to the superstructure's degrees of freedom, and x_g represents the vector of ground displacements at the supports. The vectors $\dot{x}^t, \dot{x}_g, \ddot{x}^t, \ddot{x}_g$ indicate the velocities and accelerations, respectively, and are defined analogously. P_g is the vector of forces generated at the support degrees of freedom.

The overall displacements of the superstructure and non-support degrees of freedom can be separated into relative displacements between the structure and the supports, as well as quasi-static displacements resulting from static support movements [10,11].

$$x^t(t) = x(t) + x_s(t) \tag{2}$$

The quasi-static displacements can be represented as

$$x_s = \Gamma\, x_g \tag{3}$$

Then the total displacement will be

$$x^t = x + \Gamma x_g \tag{4}$$

x_g: represents the input ground motion, while, Γ is an influence coefficient.
The displacement is separated into two components:

$$\begin{Bmatrix} x^t \\ x_g \end{Bmatrix} = \begin{Bmatrix} x_s \\ x_g \end{Bmatrix} + \begin{Bmatrix} x \\ 0 \end{Bmatrix} \tag{5}$$

To determine the quasi-static displacements x_s generated by the support displacements x_g, the quasi-static equilibrium equation can be expressed as:

$$\begin{bmatrix} K_{ss} & K_{sg} \\ K_{gs} & K_{gg} \end{bmatrix} \begin{Bmatrix} x_s \\ x_g \end{Bmatrix} = \begin{Bmatrix} 0 \\ P_g^s \end{Bmatrix} \tag{6}$$

Where, P_g^s represents the support forces required to statically enforcing displacements x_g that change over time. Furthermore, $P_g^s = 0$, if the structure is statically determinate or if the support
experiences rigid body motion, as indicated in Equation (6).

$$K_{ss}x_s + K_{sg}x_g = 0 \tag{7}$$

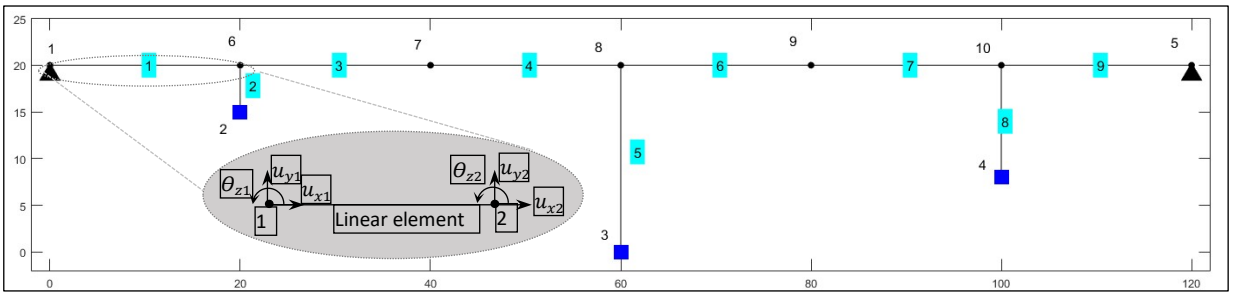

Figure 2: Finite element meshing.
Source: Authors, (2025)

Reducing the equation above by utilizing the following expression:

$$x_s = \Gamma\, x_g \tag{8}$$

$$\Gamma = -K_{ss}^{-1}K_{sg} \tag{9}$$

Replacing Equation (8) in Equation (7)

$$\left(K_{ss}\Gamma + K_{sg}\right)x_g = 0 \tag{10}$$

To determine the response of the non-support degrees of motion, the subsequent equation can be derived from Equation (1):

$$M_{ss}\ddot{x}^t + M_{sg}\ddot{x}_g + C_{ss}\dot{x}^t + C_{sg}\dot{x}_g + K_{ss}x^t + K_{sg}x_g = 0 \tag{11}$$

$$M_{ss}\ddot{x}^t + C_{ss}\dot{x}^t + K_{ss}x^t = -M_{sg}\ddot{x}_g - C_{sg}\dot{x}_g - K_{sg}x_g \tag{12}$$

In most instances, the mass coupling matrix and the damping matrix are typically of minor magnitude, resulting in minimal contribution to the overall system dynamics; hence, they can often be ignored. Consequently:

$$M_{ss}\ddot{x}^t + C_{ss}\dot{x}^t + K_{ss}x^t = -K_{sg}x_g \tag{13}$$

Next, we will substitute Equation (4) along with its corresponding velocity and acceleration components into Equation (12).

$$M_{ss}\ddot{x} + C_{ss}\dot{x} + K_{ss}x = -(M_{sg} + \Gamma\, M_{ss})\ddot{x}_g - (C_{sg} + \Gamma\, C_{ss})\dot{x}_g - (K_{sg} + \Gamma\, K_{ss})x_g \tag{14}$$

As previously derived in Equation (10), the expression $(K_{ss}\Gamma + K_{sg})x_g = 0$, and the term M_{sg}, representing the inertia coupling, can typically be disregarded for most structures. This neglect is further justified by the assumption that, for structures with mass

represented as concentrated at the degrees of freedom, the mass matrix is diagonal. This configuration implies that M_{sg} effectively becomes a null matrix, while M_{ss} retains its diagonal form. Moreover, the influence of the damping term $(C_{sg} + \Gamma\, C_{ss})\dot{x}_g$ is minimal and can also be omitted from consideration. Hence:

$$M_{ss}\,\ddot{x} + C_{ss}\,\dot{x} + K_{ss}\,x = -\,M_{ss}\,\Gamma\,\ddot{x}_g \tag{15}$$

The equation (15) is the equation of motion for the Multi Degree of freedom (MDOF) system subjected to multi-support excitation. The matrix Γ is obtained from a static analysis of structure for relative movements [12].

The finite element model utilized in this study employs a linear two-node element configuration with three degrees of freedom, as depicted in Figure 2. This figure illustrates the meshing scheme applied to the bridge, along with the node and element numbering system used in the analysis. The selection of this linear element model facilitates efficient computational analysis while capturing the essential structural behaviour of the bridge under seismic excitation.

Two excitation scenarios are applied to the horizontal components of each bridge support. In the first scenario, a uniform excitation is applied, meaning that the same ground acceleration is simultaneously exerted on all supports. In contrast, the second scenario involves a non-uniform excitation, where the same ground acceleration is applied to all supports, but with a time delay between them, as illustrated in Figure 3.b.

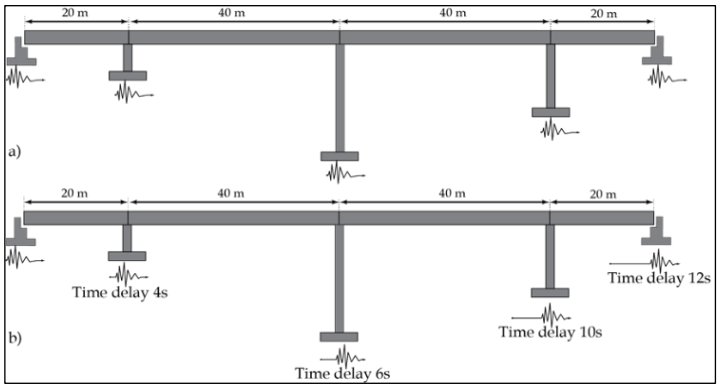

Figure 3: Excitation scenarios a) Uniform excitation , b) Non-Uniform excitation.
Source: Authors, (2025)

IV. RESULTS AND INTERPRETATIONS

In this section, we present and analyze the key results obtained from the time history analysis of the bridge under both uniform and non-uniform excitations. The discussion focuses on the maximum deformed shapes, maximum displacements, and the internal forces, including axial, shear, and bending moments. The figure 4 illustrate the maximum deformed shapes of bridge in both cases, along the duration of earthquake signal. Key Observations from this Figure:

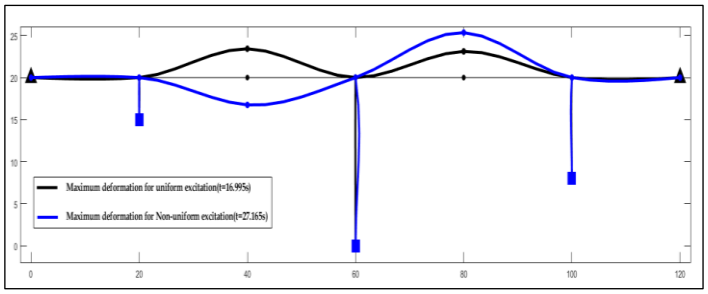

Figure 4: Maximum deformed shapes of the bridge.
Source: Authors, (2025).

• Deformation Behavior: The deformation pattern exhibits significant variation, particularly between beams 2 and 3. In the case of non-uniform excitation, the compressed and stretched fibers are reversed compared to the uniform excitation scenario. In the uniform case, both beams 2 and 3 experience compression on the bottom side. This shift directly impacts the distribution of steel reinforcement.

• Magnitude of Deformation: The magnitude of deformation under non-uniform excitation is larger compared to that under uniform excitation. This suggests the necessity of increasing the beam dimensions and the amount of reinforcement to accommodate the additional stresses.

• Temporal Shift of Peak Values: Due to the non-uniform nature of the excitation, the timing of peak structural responses shifts from 16.995 seconds to 27.167 seconds. Notably, maximum deformations occur in the final moments of the earthquake, even when the seismic intensity has substantially decreased. This highlights the importance of considering the entire duration of the earthquake during the design phase.

• Increased Flexural Demands on Central Column: The non-uniform excitation results in a greater flexural action on the central column, necessitating careful attention during the structural design to mitigate potential vulnerabilities.

• Vertical Deformation from Horizontal Excitation: Despite the horizontal application of excitation forces at the supports, the structure undergoes vertical deformation due to its elongated geometry. This behavior underscores the importance of considering structural form in the assessment of response under dynamic loading conditions.

The vertical displacement of node 9 presented in figure 5 during the earthquake period, which has the maximum values compared to other nodes

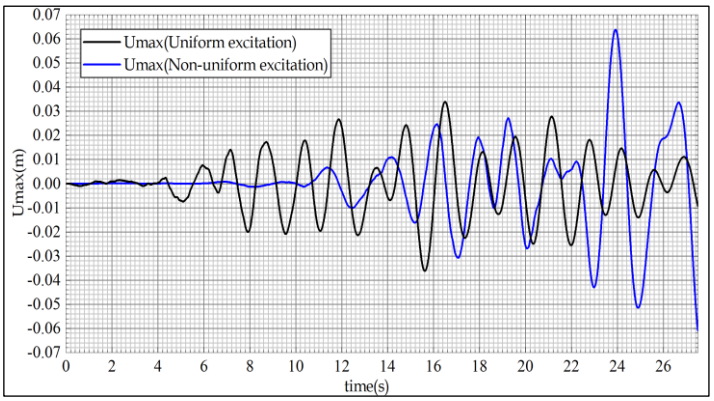

Figure 5: Vertical displacement of the node 9 during the earthquake.
Source: Authors, (2025).

The initial observation reveals a distinct variation in the response curve under non-uniform excitation. In this case, the vertical displacement remains nearly negligible until approximately the tenth second, after which it rapidly amplifies, surpassing the displacement observed in the uniform excitation case. The non-uniform excitation reaches its maximum displacement of 7.4 cm at around 24 seconds. Conversely, in the uniform excitation scenario, the vertical displacement exhibits a more harmonic pattern, reaching its peak value of 3.4 cm midway through the earthquake's duration. A comparison of these peak values demonstrates that the non-uniform excitation results in a 50% increase in maximum displacement. This significant amplification underscores the critical importance of accounting for non-uniform excitation effects in the seismic analysis of long-span structures. Figure 6 illustrates the internal forces at the middle support (number 3) during the earthquake, including axial force, shear force, and bending moment.

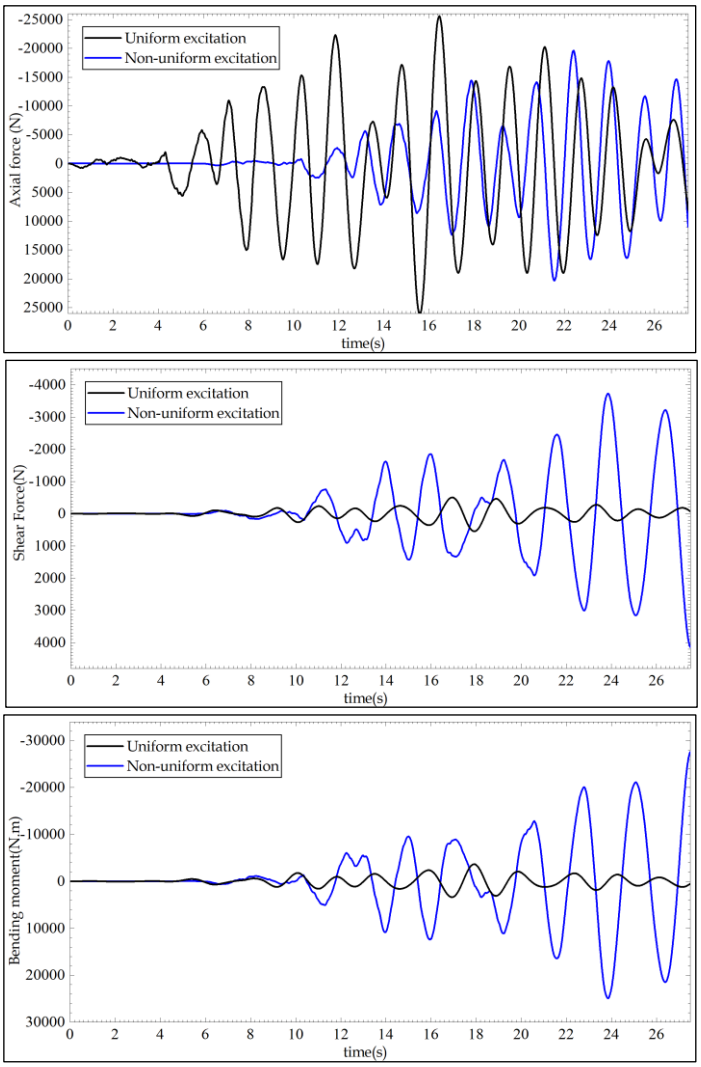

Figure 6: Internal forces at middle support N°3 during the earthquake.
Source: Authors, (2025).

In the case of non-uniform excitation, axial forces initiate oscillation at the tenth second, while under uniform excitation, the axial force exhibits greater peak values throughout. This implies that non-uniform excitation reduces the axial forces acting on the columns, potentially allowing for a reduction in column, foundation dimensions and reinforcement quantity. Conversely, the non-uniformity in excitation amplifies the shear forces by a factor of 8 and the bending moments by a factor of 6. This amplification initiates simultaneously for both excitation scenarios, indicating that the reinforcement steel required for the columns will need to be increased by 6 to 8 times compared to the uniform excitation case. The color map depicting the maximum curvature and internal forces for both cases is presented in Figure 7.

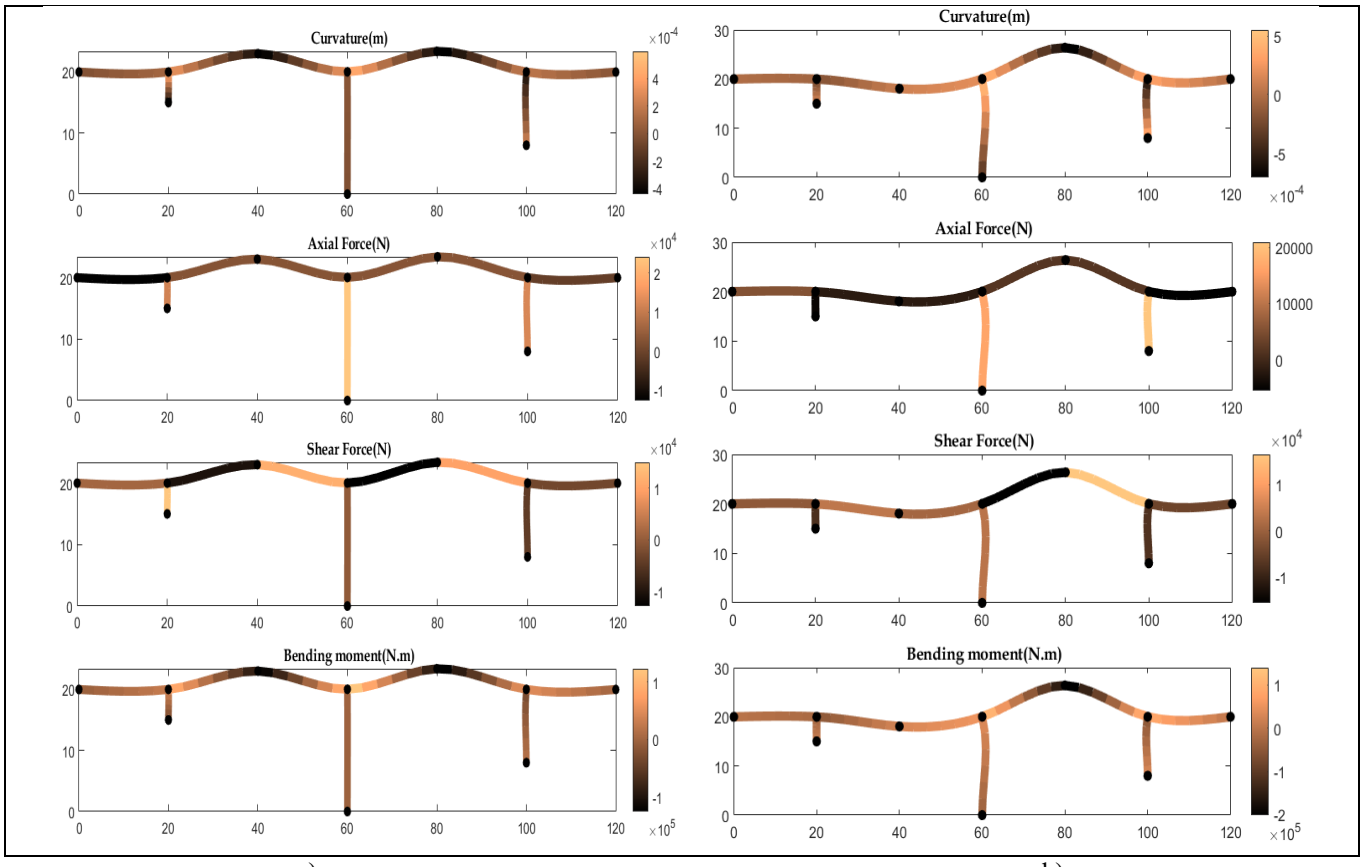

a) b)

Figure 7: Maximum curvature and internal forces for the bridge structure, a) Uniform excitation, b) Non-uniform excitation.
Source: Authors, (2025)

V. CONCLUSIONS

In conclusion, this study highlights the significant impact of asynchronous excitation on the structural response of bridges during seismic events. The key findings demonstrate that non-uniform seismic excitation results in larger deformations, a shift in the time of peak structural responses, and amplified internal forces compared to uniform excitation. Specifically, the reversal of compression and tension sides in beams under non-uniform loading alters the distribution of steel reinforcement. The increased deformations, flexural demands on central columns, and the unexpected vertical displacement of the structure despite horizontal excitation emphasize the critical need to incorporate these factors in seismic design.

For future work, there are several potential avenues of exploration. First, more sophisticated modeling techniques could be employed to capture the interaction between soil and structure under non-uniform seismic conditions, which would provide further insights into foundation and abutment behavior. Additionally, experimental validation using shake tables or field monitoring could strengthen the empirical foundation of these findings. Finally, optimizing the design of seismic isolation systems, such as lead rubber bearings, could be investigated to mitigate the effects of non-uniform excitation and enhance the overall seismic resilience of long-span bridges.

VI. AUTHOR'S CONTRIBUTION

Conceptualization: Guesmi Mohamed, Belkheiri Nassira and Guesmi Mohamed Lakhder.
Methodology: Guesmi Mohamed, Belkheiri Nassira and Guesmi Mohamed Lakhder.
Investigation: Guesmi Mohamed, Belkheiri Nassira and Guesmi Mohamed Lakhder.
Discussion of results: Guesmi Mohamed, Belkheiri Nassira and Guesmi Mohamed Lakhder.
Writing – Original Draft: Guesmi Mohamed, Belkheiri Nassira and Guesmi Mohamed Lakhder.
Writing – Review and Editing: Guesmi Mohamed, Belkheiri Nassira and Guesmi Mohamed Lakhder.
Resources: Guesmi Mohamed, Belkheiri Nassira and Guesmi Mohamed Lakhder.
Supervision: Guesmi Mohamed, Belkheiri Nassira and Guesmi Mohamed Lakhder.
Approval of the final text: Guesmi Mohamed, Belkheiri Nassira and Guesmi Mohamed Lakhder.

VIII. REFERENCES

[1] A. Zerva, Spatial Variation of Seismic Ground Motions: Modeling and Engineering Applications. CRC Press, 2009. https://doi.org/10.1201/97814200 09910.

[2] S. Yadi, B. Suhendro, H. Priyosulisty, and A. Aminullah, "Dynamic response of long-span bridges subjected to non-uniform excitation: A state-of-the-art review," MATEC Web Conf., vol. 258, p. 05017, 2019. https://doi.org/10.1051/matecconf/ 201925805017.

[3] A. G. Sextos, A. J. Kappos, and K. D. Pitilakis, "Inelastic dynamic analysis of RC bridges accounting for spatial variability of ground motion, site effects and soil-structure interaction phenomena," Earthq. Eng. Struct. Dyn., vol. 32, no. 4, pp. 629–652, 2003. https://doi.org/10.1002/eqe.246.

[4] S. Hoseini, M. Davoodi, and M. Kamal, "The effect of foundation soil behavior on seismic response of long bridges," Geomech. Eng., vol. 17, no. 6, pp. 583–595, 2019. https://doi.org/10.12989/gae.2019.17.6.583.

[5] M. Yurdakul and S. Ateş, "Effectiveness of wave passage effect of seismic isolated and nonisolated bridges under spatially varying ground motion," Eng. Sci., vol. 13, no. 3, pp. 201–221, 2018. http://dx.doi.org/10.12739 /NWSA.2018.13.3.1A0415.

[6] A. Amin, M. Islam, and M. J. Ahamed, "Base isolation of multi-storied building using lead rubber bearing," Journal of Engineering and Technology for Industrial Applications, vol. 6, no. 26, pp. 52–60, Nov./Dec. 2020. https://doi.org/10.5935/ jetia.v6i26.697

[7] J. Shen, X. Ren, and J. Chen, "Effects of spatial variability of ground motions on collapse behaviour of buildings," Soil Dyn. Earthq. Eng., vol. 144, p. 106668, 2021. https://doi.org/10.1016/j.soildyn.2021.106668.

[8] P. Ering and S. Babu, "Effect of spatial variability of earthquake ground motions on the reliability of road system," Soil Dyn. Earthq. Eng., vol. 136, p. 106207, 2020. https://doi.org/10.1016/j.soildyn.2020.106207.

[9] M. Guesmi, N. Belkheiri, and M. L. Guesmi, "Time history analysis of structures under multi-support excitation by state-space method," Stud. Eng. Exact Sci., vol. 5, no. 1, pp. 209–222, 2024. https://doi.org/10.54021/seesv5n1-012.

[10] A. K. Chopra, Dynamics of Structures: Theory and Applications to Earthquake Engineering. Pearson, 2014.

[11] T. K. Datta, Seismic Analysis of Structures. Wiley, 2010.

[12] R. Clough and J. Penzien, Dynamics of Structures. McGraw-Hill, 2003.